

Application of rheological measurements for probing the sedimentation of suspension concentrate formulations†

Malcolm A Faers* and Graham R Kneebone

AgrEvo UK Ltd, Hauxton, Cambridge CB2 5HU, UK

Abstract: In this paper, the role of both non-adsorbing (depleting) and adsorbing (stabilizing) polymers is investigated in the process of sedimentation in aqueous suspension concentrates. A range of polymers with different molecular masses have been used. By measuring the rheology of these systems and also studying the sedimentation of model polystyrene latex and real agrochemical suspensions of fluquinconazole, we have observed that the sedimentation rate is related to the nature of the particle flocs and that the rate of sedimentation is significantly reduced once a continuous network of particles is formed. Rheologically this corresponds to the formation of a weak elastic gel. When the attraction between particles is sufficient, this network is formed via a diffusion-limited aggregation mechanism, has an open structure and sediments slowly. The network, however, is able to rearrange into a more dense reaction-limited structure which sediments more rapidly. This transition from a slow to a faster sedimentation rate takes up to four days and depends on the strength of the attraction between the particles, the volume fraction of particles and molecular mass of the non-adsorbing polymer. Soft adsorbed polymer stabilizing layers lead to weaker flocculation, require more non-adsorbing polymer for network formation and could result in more rapid sedimentation.

A range of suspensions containing different molecular mass non-adsorbing polymers and with the same sedimentation rate have different rheologies, including the zero shear viscosity. Consequently, the flocculated network is not the only factor in sedimentation and the non-adsorbing polymer also contributes. Furthermore, there is no direct correlation between rheology and sedimentation. This difference could be due to the non-adsorbing polymer molecules having to diffuse through the network of particles before the particle clusters in the network can rearrange and sedimentation occur.

© 1999 Society of Chemical Industry

Keywords: suspension concentrate; sedimentation; rheology; flocculation; xanthan

1 INTRODUCTION

Suspension concentrates (SC) are an important formulation type in the design of crop protection products and are one of the vehicles through which an active ingredient is applied to its target crop by the farmer in a stable, safe and biologically active form. Typically, a simple suspension concentrate is composed of an insoluble, micron-sized, crystalline dispersion of one or more pesticides, suspended in a liquid, usually aqueous, medium. Surfactants are also incorporated to wet and disperse the particles, which can combine both steric and electrostatic stabilization. However, in order to maintain its potency, a suspension concentrate must be stable to any change over its lifetime, which may extend for up to three years. For example, there must be no significant chemical degradation of the active ingredient(s) and no irreversible sedimentation of the dispersed

phase. The latter, if not controlled by an anti-settling agent, can lead to dilatant layers i.e. layers which become more viscous when subjected to shear, and so are difficult to redisperse.

Sedimentation can be particularly acute in agricultural suspension concentrates where a balance of properties is required. A suspension needs to be sufficiently viscous to prevent sedimentation and yet also be sufficiently fluid to allow it to be readily emptied and rinsed from its pack. This is often achieved by the addition of polymers or clays which form gels that are sufficiently strong to overcome gravitational stresses and prevent sedimentation. However, upon application of a slightly greater stress, such as encountered when inverting the pack or pouring out the contents, the 'gel' must be sufficiently weak such that it breaks down and allows the suspension to flow. Rheologically this corresponds to

* Correspondence to: Malcolm A Faers, AgroEvo UK Ltd, Hauxton, Cambridge CB2 5HU, UK
E-mail: malcolm.faers@agroevo.com

† Based on poster presentations at the 9th International Congress

of Pesticide Chemistry, organised by the International Union of Pure and Applied Chemistry (IUPAC), and held in London, UK, 2–7 August 1998.

(Received 10 July 1998; accepted 30 October 1998)

a 'solid' on standing which breaks down to a fluid on application of a stress or with shearing, ie a plastic material. It is this high degree of shear-thinning which is required to satisfy both requirements simultaneously.

Xanthan, a polysaccharide produced by the micro-organism *Xanthomonas campestris*,¹ is commonly used as an anti-settling agent in concentrated suspensions in the agrochemical and other industries on account of the highly elastic nature of its aqueous solutions on standing and their high degree of shear-thinning under applied stresses or strains.

Although a large amount of work has been carried out on the properties of aqueous xanthan solutions there appears to be very little literature describing work on xanthan gum-thickened suspensions, with different views emerging as to the mechanism by which xanthan inhibits sedimentation. For example, Clark and Lockwood² have suggested that it is the high viscosity of the gel-like xanthan solutions which retards the sedimentation of any particles suspended in it. In contrast, Howe and Robins³ have reported that the addition of xanthan to non-ionic-stabilized oil-in-water emulsions results in their flocculation by a depletion mechanism and a reduction in the rate of creaming. This suggests that the xanthan may also flocculate suspensions in a similar manner and that it may be the flocculated network of particles which prevents sedimentation rather than the high viscosity of the xanthan gel. Wedlock *et al*⁴ posed this very question when they studied the sedimentation profiles of xanthan-thickened suspensions. However, they were unable to answer it unequivocally.

Three distinct types of sedimentation in suspensions, namely those of dispersed, aggregated and reversibly flocculated dispersions, have been identified and comprehensively reviewed by Buscall.⁵ In the first case, the sedimentation of monodisperse, dispersed systems has been much studied and is well understood. Here the particles sediment individually according to Stokes' law with a correction for dispersed phase volume due to Kynch.⁶ Richardson and Zaki⁷ empirically correlated the sedimentation rate for hard spheres and found that they were described by the following relationship:

$$\frac{U_s}{U_t} = (1 - \phi)^\beta \quad (1)$$

where U_s is the sedimentation rate of the suspension, U_t is the sedimentation rate of a single particle at infinite dilution and $\beta = 5$ at the limit of slow sedimentation where the particle's drag is given by Stokes' law, which is the case with colloidal suspensions. This correlation has been confirmed both for a wide range of volume fractions⁸ and for colloidal-sized polystyrene latices and silica particles with β values of $c 5.4$.⁵ Rheologically, these systems normally exhibit Newtonian flow at very low volume fractions and pseudoplastic flow at higher concentra-

tions, with this behaviour originating from the inter-particle and Brownian forces at low shear rates and the hydrodynamic flow of the medium around the particles at high shear rates.

Aggregated systems are very different and form a continuous network of permanently flocculated particles. Since the particles are locked into the network they cannot sediment in the true sense of the word. Here, the structure 'consolidates' at its base if the weight of the whole flocculated structure above is sufficient to overcome the strength of the individual bonds between the particles, ie the network yields. Michaels and Bolger⁹ described this in terms of a compressive yield stress, P_y , which must exceed the static stress at the base of the network, P_s , for consolidation to occur. The static stress at the base of the network is given by:

$$P_s = \Delta\rho g H_0 \phi_0 \quad (2)$$

where $\Delta\rho$ is the density difference between the dispersed and continuous phases, g is the acceleration due to gravity, H_0 is the initial height of the network and ϕ_0 is the initial volume fraction of the dispersed phase. It can clearly be seen that the rate of consolidation depends not only on the effective weight of the network but also on the height of the sample, and that consolidation continues only until the weight of the structure is balanced by the strength of the inter-particle bonds. However, in order for consolidation to occur, the network must also shear at the walls and, as for the compression case, the wall shear stress, σ_y , must exceed the static stress at the wall, σ_s , which is given by:

$$\sigma_s = \frac{\Delta\rho g \phi_0 d}{4} \quad (3)$$

where d is the diameter of a cylindrical container. Therefore, consolidation also depends on the diameter of the container and for sufficiently narrow tubes the contribution from the walls may be so great that consolidation will not occur. Michaels and Bolger studied the effect of container height and diameter with kaolin slurries and found that the consolidation rate depended strongly on height, while diameter had little effect. This was confirmed by Buscall⁵ with polystyrene latices where P_y was some 40 to 1000 times greater than σ_y . Rheologically these systems are gel-like and exhibit plastic flow with a yield stress, below which the sample does not flow. Examples of such systems include clay dispersions and aqueous latices coagulated by electrolyte.^{9,10}

Finally, there is the case for reversibly flocculated dispersions, where the particles are weakly flocculated and rearrange their structure on the same time-scale as sedimentation. These systems lie between dispersed and aggregated systems and are more complex to study, showing both true sedimentation and consolidation, and pseudoplastic or plastic

behaviour rheologically. Accordingly, such systems have received limited attention amongst researchers. Buscall and McGowen¹¹ studied the behaviour of a 1- μm polystyrene latex weakly flocculated, probably through bridging, by sodium carboxymethylcellulose (NaCMC). Despite being flocculated, pseudoplastic flow was observed and there appeared to be no minimum gravitational stress below which sedimentation did not occur. Also, when suitably scaled, the sedimentation rate measured as a function of centrifugal acceleration correlated with the shear flow rate measured as a function of applied shear stress. This suggested that shear stress and gravity were having similar effects on the structure. In a study of weakly flocculated latex, Partridge¹² showed that, at high concentrations, sedimentation occurred after a delay time. This indicated that the structure was changing with time.

Weakly flocculated suspensions may also be achieved through depletion flocculation by the addition of a non-adsorbing polymer. Above a certain concentration of polymer, depletion flocculation can create a structure capable of resisting sedimentation. Tadros and Zsednai¹³ used hydroxyethylcellulose (HEC) to prevent the formation of dilatant sediments in an aqueous suspension of the fungicide ethirimol. Addition of HEC resulted in depletion flocculation of the particles into a rigid three-dimensional network which was able to resist sedimentation under gravitational stress. Interestingly, this mechanism for preventing sedimentation was considered to be different from the effect caused by xanthan. Buscall *et al*¹⁴ studied the sedimentation of polystyrene latices in HEC solutions, where they found that the sedimentation was governed by the zero

shear viscosity. However, the authors were interested in the sedimentation of stable dispersions and obtained their findings at low latex volume fractions (≤ 0.05) where the formation of a flocculated network is unlikely. At the other extreme at high volume fractions, Wedlock *et al*¹⁵ measured the consolidation rates of a herbicide suspension in xanthan and succinoglycan solutions. The latter, which showed the least separation, also exhibited no yield stress rheologically but a low-shear Newtonian plateau at low shear stresses. The authors inferred from this that the resistance to sedimentation arises from the very high resting viscosities and not from a yield stress which inhibits particle movement.

However, sedimentation in agricultural suspensions is a complex area that exhibits unexpected behaviour. For example, in Fig 1 it can be seen how non-aqueous SCs containing a flocculated clay structuring agent sediment at a rate proportional to their height, as would be predicted for a consolidating network, whereas aqueous SCs containing xanthan show no such height dependence. The following work examines the mode of action by which xanthan inhibits the sedimentation of agricultural suspension concentrates.

2 EXPERIMENTAL

Polystyrene latices in the 70 and 450 nm size range were prepared by the dispersion polymerisation of styrene according to the method of Goodwin *et al*^{16,17} as described previously.^{18,19} These were stabilized with adsorbed ABA block copolymers (Synperonic PE range, ICI) of poly(ethyleneoxide)-poly(propyleneoxide)-poly-(ethyleneoxide) (PEO-

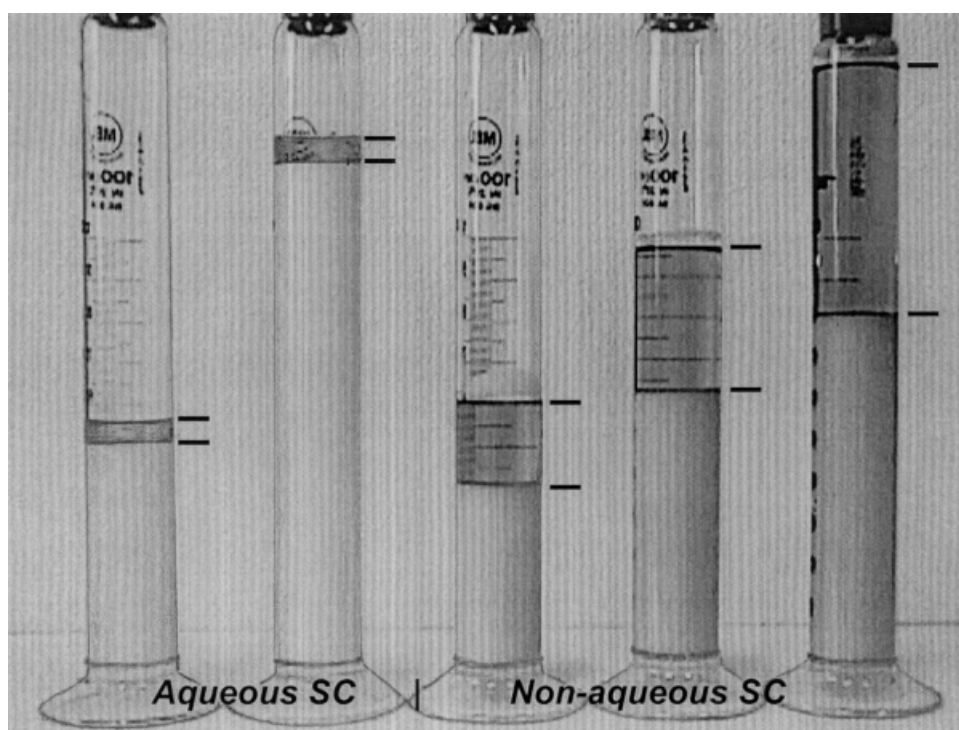


Figure 1. Height effects during sedimentation with (left) aqueous and (right) non-aqueous suspension concentrates.

PPO-PEO) at full monolayer coverage. The size of each latex was determined from photon correlation spectroscopy.

HEC (Natrosol 250 grades) and xanthan (Kelzan grade) were obtained from Hercules UK Ltd and Kelco Biopolymers (a unit of Monsanto plc), respectively. These polymers were purified by dialysis against distilled water for at least two weeks, by which time the conductivity had dropped to $10^{-5} \text{ S cm}^{-1}$. A small quantity of formaldehyde was added to prevent microbial degradation. The molecular characteristics of all these polymers are given in Table 1.

Suspensions of fluquinconazole (a hydrophobic crystalline fungicide, mp 192°C , density 1.58 g cm^{-3}) were prepared by milling a 500 g kg^{-1} suspension with Synperonic PE/P103 (20 g litre^{-1}) in an Eiger 250 bead mill to give a Sauter mean diameter of $1.47 \mu\text{m}$. This quantity of P103 was considered more than adequate to give full coverage of fluquinconazole.

All experiments were performed in 10 mm sodium chloride at neutral pH to ensure that the interactions between the particles were essentially steric in nature. The electrolytes used in this study were analytical grade materials and were used without further purification. The water used was deionized and distilled or of similar quality.

Sedimentation experiments were performed in 100-ml glass measuring cylinders (26 mm internal diameter) or glass test tubes (13 mm internal diameter). The height of samples in these tubes was typically 130 mm for the fluquinconazole suspensions (stored in cylinders) and 70 mm for the latex samples (stored in test tubes). During sedimentation, samples were maintained in a thermostatted room at $20\text{--}25^\circ\text{C}$.

2.1 Rheological experiments

In order to optimize the properties of agricultural suspensions and predict how they will behave, it is necessary to understand the mechanism by which they resist sedimentation under gravitational stresses. In this respect, rheology is a useful tool for probing the interactions that govern this behaviour. However, for measurements to provide information on the structure which exists within SCs it is necessary to perform experiments (eg oscillation, stress

relaxation/creep) at very low deformations below the point at which the structure starts to break down. The experiments were carried out using a Bohlin VOR Rheometer (Bohlin Instruments Ltd, Cirencester, UK) at 20°C with either couette or double gap measurement geometries.

2.2 Shear rate sweep viscometry

In this experiment the suspension is sheared over a wide range of shear rates (eg 10^{-3} to 10^3 s^{-1}). The outer cylinder is rotated at known shear rates, $\dot{\gamma}$, and the resulting stress, σ , transmitted through the sample to the inner cylinder is measured through the displacement of a stiff torsion spring. Hence, the viscosity, η , which is given by:

$$\eta = \frac{\sigma}{\dot{\gamma}} \quad (4)$$

can be measured as a function of shear rate. Unfocculated suspensions typically exhibit Newtonian or pseudoplastic flow over the experimentally accessible shear rate range. However, focculated suspensions exhibit plastic flow with a yield stress, which was interpreted in terms of the Bingham model:

$$\sigma = \sigma_y + \eta\dot{\gamma} \quad (5)$$

where σ_y is the Bingham yield stress. This is an extrapolated yield stress obtained from the high-shear Newtonian region which is typically at shear rates of $10^2\text{--}10^3 \text{ s}^{-1}$ and corresponds to the force required to fully break down the focculated structure.

For focculated suspensions, the yield stress is a measure of the energy required to separate aggregates. Therefore, the yield stress divided by the total number of particle-particle contacts is the energy required to separate two focculated particles, E_{sep} ^{20,21}

$$E_{\text{sep}} = \sigma_y \frac{8\pi a^3}{3\phi n} \quad (6)$$

where n is the average number of contacts per particle. The upper and lower extremes are 12 for hexagonal close packing and 2 for a chain. For this work

Table 1. Properties of polymer materials used in this work

Series	Grade	Polymer type	Approximate relative molecular mass	EO (% w/w)
Synperonic PE	P103	PEO-PPO-PEO block copolymer	4950	30
	P105	PEO-PPO-PEO block copolymer	6500	50
	F108	PEO-PPO-PEO block copolymer	14 600	80
Natrosol 250	L	HEC	0.085×10^6	—
	G	HEC	0.3×10^6	—
	M	HEC	0.7×10^6	—
	HHX	HEC	1.0×10^6	—
Kelzan	—	Xanthan	2.0×10^6	—

a value of 4 was chosen. It is this uncertainty regarding n which makes it difficult to determine the strength of the inter-particle attraction from rheological measurements, since the yield stress also depends strongly on the openness of the flocs.

2.2 Oscillatory shear

The second mode of operation is oscillatory shear in which a sinusoidally varying strain of known amplitude (γ_0) is applied and the resulting sinusoidal stress (amplitude σ_0) is measured. From these we can define the complex modulus, G^* ;

$$G^* = \frac{\sigma_0}{\gamma_0} \quad (7)$$

On account of the viscoelasticity which exists in samples, the stress is shifted out of phase by an angle, θ , but has the same frequency dependence. Therefore, the complex modulus can be split into two parts, the elastic modulus, G' , and the viscous modulus, G'' . These are related to the phase angle, θ , by:

$$G' = G^* \cos \theta \quad (8)$$

$$G'' = G^* \sin \theta \quad (9)$$

It is important to note that the moduli are all frequency-dependent. For a Newtonian fluid $\theta = \pi/2$ and for a Hookean solid $\theta = 0$, with viscoelastic materials having a phase angle between these two limits.

These three moduli must be measured in the linear viscoelastic region where the rheological parameters are independent of the amplitude. Therefore, a strain sweep, where the applied strain at one frequency (0.5 Hz) is gradually increased, is performed for each dispersion to ensure operation in the linear viscoelastic region. Once this has been defined, measurements are carried out as a function of frequency (10^{-2} –10 Hz) below this critical strain, γ_c , where the structure begins to break down.

Flocculated networks are generally elastic in nature with $G' > G''$. Here it is the flocs which span the rheometer cell that transmit the deformation through the sample. Therefore, in this respect, G' can be regarded as a measure of the number of 'chains' that permeate through the floc network. This is illustrated in Fig 2.

Likewise, if measurements are performed with a flocculated network as a function of increasing strain, then the chains will tend to straighten elastically (like a spring) until they rupture at full extension. Here, the critical strain or elastic limit can be regarded as a measure of the 'tortuosity' of the floc network. This is illustrated in Fig 3.

In reality, this is a vast simplification of the structure that exists in flocculated suspensions but serves as a useful illustration to aid interpretation of such

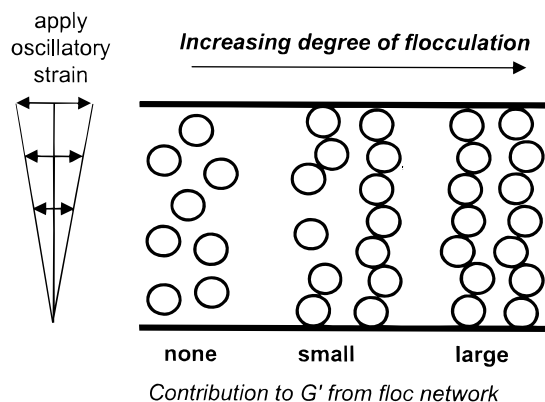


Figure 2. Illustration of the relationship between the floc network structure and elastic modulus, G' .

measurements. For actual flocculated suspensions, the floc network will be composed of individual particles flocculated into clusters of various sizes which in turn are flocculated into larger clusters or continuous networks.

2.3 Stress relaxation

This experiment is also a measure of the elasticity which exists within samples and as such can only be used for viscoelastic or elastic samples. Here, a strain (within the linear viscoelastic region) is rapidly applied and maintained at a constant level while the stress is monitored as a function of time. The stress at time t , $\sigma(t)$, divided by the constant strain, γ_0 , gives the relaxation modulus, $G(t)$:

$$G(t) = \frac{\sigma(t)}{\gamma_0} \quad (10)$$

At sufficiently short times, $G(t)$ corresponds to the elastic limit, G^∞ , while, at longer times, the stress can either relax to zero, in which case the sample is viscoelastic and has a zero shear viscosity, η_0 , which can be obtained from:

$$\eta_0 = \int_0^\infty G(t) dt \quad (11)$$

or the stress can decay to a constant value at long times, in which case the sample is an elastic solid and

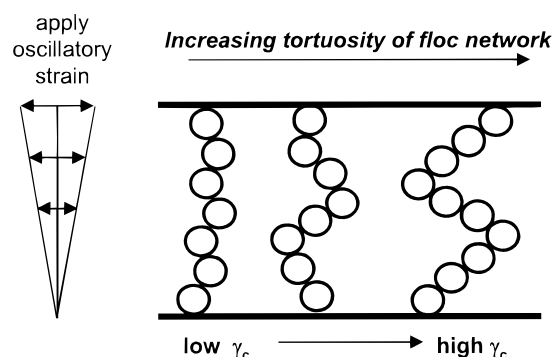


Figure 3. Illustration of the relationship between the floc network structure and critical strain or elastic limit.

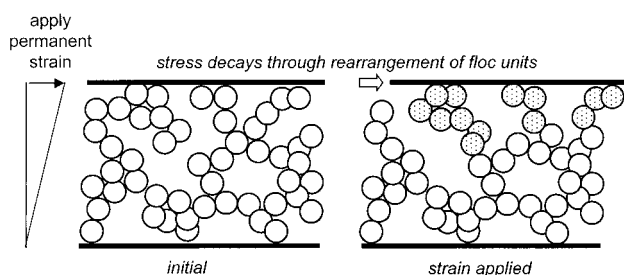


Figure 4. Illustration of how stress decays in stress relaxation experiments through the rearrangement of floc units within the network.

has an infinite viscosity. This long-term stress corresponds to the yield stress of the sample at very long times and the existence of such a value would indicate that a sample is likely to sediment through a consolidation mechanism (ie show height dependence and collapse at its base).

With flocculated suspensions, this experiment basically measures the time taken for individual clusters in the floc to rearrange and is illustrated in Fig 4. Accordingly, it is a good measure of the persistence of the network structure and perhaps a good indication of how quickly a network may rearrange when sedimenting. This experiment is equivalent to creep measurements available with controlled-stress rheometers.

The shear history can also be important, especially in the case of flocculated suspensions. Therefore, to ensure a common history, each sample was measured beyond its elastic limit with a sinusoidal strain at 0.5 Hz and then monitored within its linear viscoelastic region as a function of time until the structure reformed. In all cases this was found to be a rapid process, of the order of seconds, and with little long timescale dependence.

3 RESULTS AND DISCUSSION

3.1 Effect of non-adsorbing polymer concentration

One particularly informative experiment involved the addition of increasing levels of a non-adsorbing polymer (xanthan) to polystyrene latex. In Fig 5, a series of tubes containing 482-nm latex particles dispersed in water at a volume fraction of 0.16 are shown at increasing xanthan contents (shown on the tubes). These samples have been allowed to sediment for about one month. The results can be split into three distinct zones:

Zone A: a homogeneous, white, opaque suspension with a diffuse interface at the sediment-supernatant boundary.

Zone B: rapid sedimentation occurs, iridescence is observed in the sediment, the supernatant is clear and the interface is sharp.

Zone C: little sedimentation occurs, the supernatant is clear, the interface is sharp and no iridescence is seen.

What we are seeing here is the effect of gradually increasing the strength of the attraction between the particles through depletion flocculation and may be described accordingly for each zone:

Zone A: without any HEC the particles are dispersed and remain suspended due to their thermal energy.

Zone B: with small attractive forces, the particles associate into small aggregates which sediment rapidly. These small aggregates are relatively compact (ie have a high fractal dimension) and, from the iridescence present, appear to have regular order. The presence of a sharp interface and clear supernatant indicates that all the particles are flocculated.

Zone C: with higher attractive forces, the particles arrange themselves into relatively open flocs (ie have a low fractal dimension) which have the ability to form a network which effectively spans the sample. These states of aggregation of the latex particles are illustrated for each zone.

It is the presence of the particulate network in zone C that prevents the suspension from sedimenting. This can be clearly seen in the graphs of the sedimentation rate and elastic modulus, G' , shown below the tubes. Here, the formation of an elastic network ($G' > G''$) corresponds to the point where there is a sharp reduction in the sedimentation rate. This change in the state of the dispersion can also be seen microscopically; in zone A particles are uniformly distributed and mobile (ie dispersed) while in zone C the particles are aggregated.

The mechanism for this flocculation is consistent with depletion, for example, when a sample in zone C is mixed with a xanthan-free latex sample such that the resulting xanthan concentration is less than that required for flocculation, a dispersed suspension is produced. Depletion flocculation arises from an imbalance in osmotic pressure which occurs when polymer molecules are excluded from the region between two particles when their surface separation is less than the diameter of the polymer coil.^{22,23} However, for depletion flocculation to occur it is necessary for the polymer molecules to be repelled from the surface. Gast *et al*²⁴ and Wedlock *et al*⁴ have shown that this is the case with poly(ethyleneoxide)-based non-ionic surfactants, which prevent adsorption of hydroxyethylcellulose (HEC). This also appears to be the case for xanthan, with no signs of adsorption occurring in the presence of the adsorbed surfactant layer of P105. It is this flocculation in SCs which results in a sharp interface between the sediment and supernatant, even when a wide distribution in particle sizes exists (as in Fig 1).

3.2 Latex volume fraction effects

This time, the depleting polymer concentration (HEC M) has been fixed and the volume fraction of the latex (ϕ) increased. The displacement of the

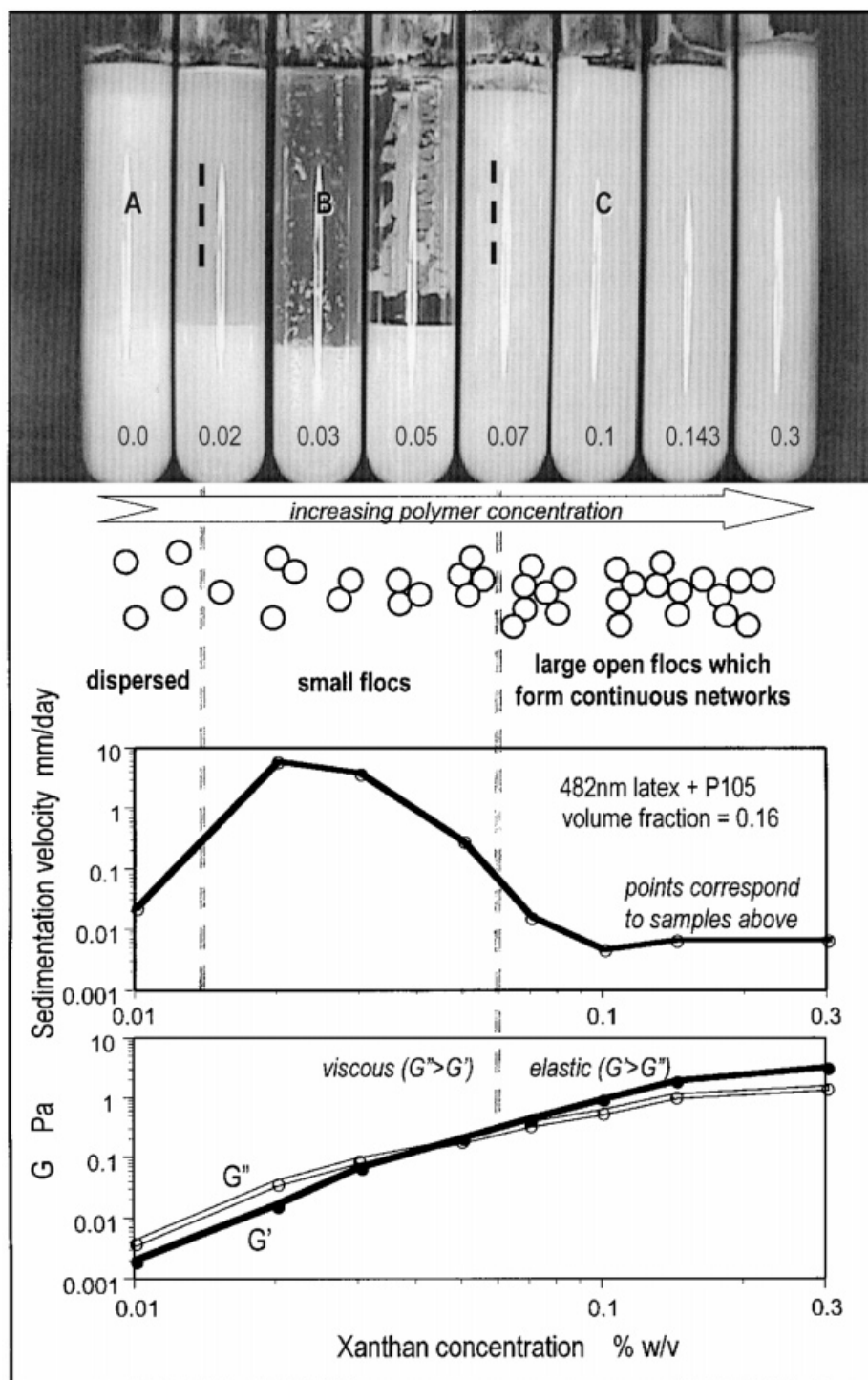


Figure 5. Sedimentation in a 482 nm latex containing xanthan, with sedimentation velocities and oscillatory moduli for each sample.

supernatant–sediment interface with time from its initial height is shown in Fig 6. For certain volume fractions, two sedimentation rates can be observed, an initial slower rate and a long time faster rate. In some samples (eg $\phi = 0.1$), this transition can take up to four days to occur. This appears to be due to a rearrangement of the floc structure from an open network to one that is more compact. This is a consequence of the strength of the attractive forces between particles.

When these are high, approaching particles will stick immediately on contact, forming a relatively

open floc or a ‘diffusion limited aggregate’ (DLA). These flocs have a low fractal dimension of 1.8 and correspond to the diffusion-limited cluster–cluster aggregation model of Meakin²⁵ and Kolb *et al.*²⁶

However, when the attractive forces are low, the particles can explore several configurations prior to aggregation, resulting in a ‘reaction limited aggregate’ (RLA). These flocs have a higher fractal dimension of 2.1 and correspond to the reaction-limited cluster–cluster aggregation model according to Brown and Ball.²⁷ Examples of these are illustrated in Fig 7.

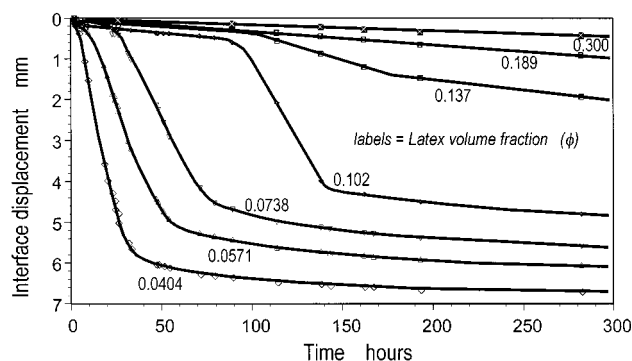


Figure 6. Sedimentation profiles for a 482 nm latex at increasing volume fractions in 3.0 g litre⁻¹ HEC M.

Rheology can help us here, in that the fractal scaling can be related to the elasticity of a suspension thus:^{10,27}

$$\text{For DLA} \quad G' \propto \phi^{3.5}$$

$$\text{For RLA:} \quad G' \propto \phi^{4.5}$$

Figure 8 shows a log-log plot of the elastic modulus against latex volume fraction for three different concentrations of HEC. The slope corresponds to the scaling for DLA or RLA processes. At the lowest HEC concentration, 0.14%, a scaling of 4.3 is obtained, in good agreement with RLA, while, for the higher HEC concentrations, the scaling is in agreement with DLA.

Consequently, where the inter-particle forces are not too strongly attractive, particles can initially flocculate into a DLA structure. Then, with time, the

floc structure rearranges into the more dense RLA structure which is less capable of resisting gravitational stresses and, hence, sediments more rapidly. At higher attractive forces, the structure becomes locked into the DLA arrangement and only one sedimentation rate is observed. Such a rearrangement was also observed by Sonntag and Russel²⁸ with electrostatically stabilized latices which were flocculated into gels. Initially, these gels had a value of 2.5, indicating an open, diffusive-type network. However, after ageing for up to 15 weeks, this scaling had increased to 4.5, in keeping with the formation of a more dense reaction-limited network.

In Fig 9, the sedimentation rates for the data in Fig 6 are plotted. For latex volume fractions up to about 0.15, two rates are visible and above this concentration, one rate. This tells us that the concentration of flocs in the suspension is also important: if each floc is too tightly constrained by its neighbours, then it cannot rearrange its structure from that of a diffusion-limited network to that of a reaction-limited network.

3.3 Effect of steric stabilizing layer softness

Since it appears that the formation of a flocculated network of particles is responsible for controlling the sedimentation of polymer-thickened suspensions, then it is fair to expect the inter-particle forces also to have an effect on the network properties. This has been reported recently,¹⁸ where the softness of a steric stabilizing layer was investigated. In this study, a relatively small, monodisperse polystyrene latex (67 nm diameter, core volume fraction 0.16) was stabilized separately by three different PEO-PPO-PEO block copolymers with equal PPO contents but different amounts of PEO, and flocculated, through the depletion mechanism, by non-adsorbing HEC (molecular mass = 0.3×10^6).

An interesting feature of these systems was the presence of a 'liquid' phase in equilibrium with a 'gas' phase and even a three-phase region which contained coexisting 'gas', 'liquid' and 'solid' phases, as

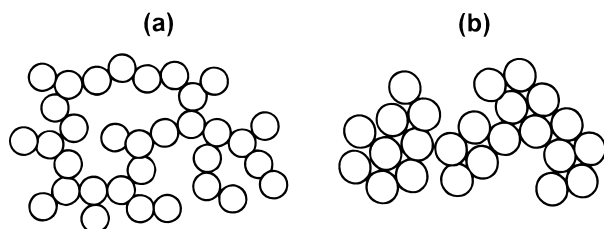


Figure 7. Illustration of (a) diffusion-limited cluster-cluster aggregated network and (b) reaction-limited cluster-cluster aggregated network.

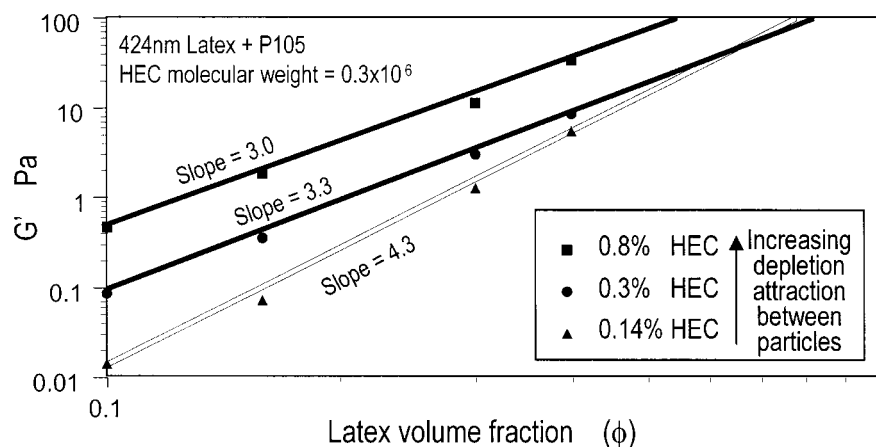


Figure 8. Scaling properties of elastic modulus as a function of volume fraction for a 424 nm latex in HEC G.

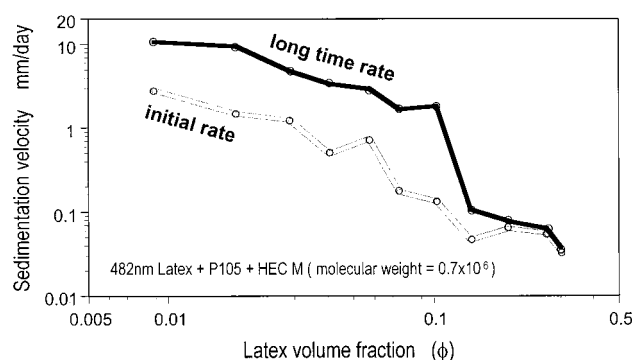


Figure 9. Sedimentation rates for the data shown in Fig 6.

modelled by Lekkerkerker *et al*²⁹ for systems where the ratio of non-adsorbing polymer coil size to particle size is greater than 0.3.

These phase properties enabled a phase diagram to be constructed from microscopic observations (see Fig 10) which revealed the effect of the particle softness on the phase boundaries. The onset of the different phase boundaries with HEC concentration scaled inversely with the chain length of the PEO adsorbed at the interface ie F108 > P105 > P103.

Rheological measurements can yield useful information. In Fig 11 the elastic modulus in the linear viscoelastic region at a frequency of 0.5 Hz is plotted for the three stabilizing copolymers as a function of HEC concentration. The elastic modulus initially rises sharply and then plateaus at higher HEC concentrations. The increase in modulus is a result of the particles flocculating to form a three-dimensional network which transmits the applied strain through the sample. Furthermore, the value of G' is proportional to the number of these 'chains' that permeate through the sample, as illustrated in Fig 2. That a plateau is observed suggests that, once the network is formed, its structure does not change with further HEC addition, as shown by the constant value of G' between 0.8 and 1.6% HEC. This would be consistent with the formation of a DLA structure. Furthermore, identical plateau values are obtained for each of the stabilizing polymers, indicating that the floc structures for each copolymer are similar.

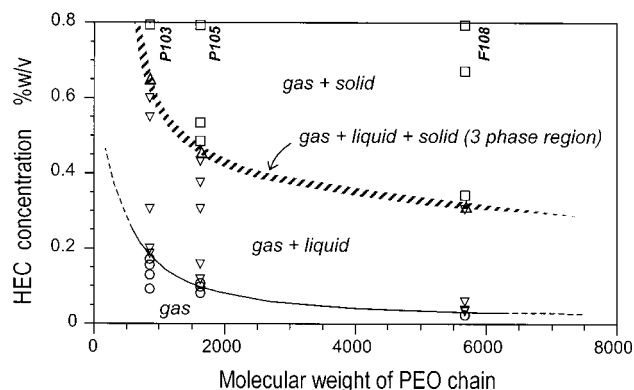


Figure 10. Phase diagram determined from microscopic observations for a 67 nm latex at a core volume fraction of 0.16 in HEC G.

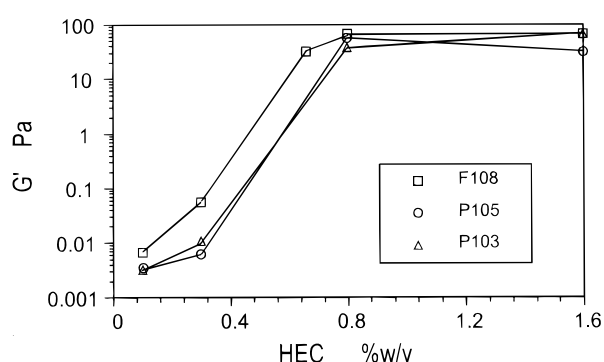


Figure 11. Elastic modulus (0.5 Hz) as a function of HEC G concentration for a 67 nm latex stabilized with different PEO-PPO-PEO block copolymers.

There is an indication with these results that the flocculated network forms at a lower HEC concentration with F108, which has the longest poly(ethyleneoxide) chain. However, to more fully characterize the floc structure, information is also required on the elastic strain limit of the samples.

In Fig 12, the critical strain for the flocculated latices is shown. As for the elastic modulus, no differences are apparent between the different copolymers, implying that the stabilizing layer has no effect on the tortuosity of the floc structure. However, the critical strain does increase slowly with increasing HEC content, implying that the structure does become more tortuous with increasing HEC concentration. From these oscillation results it can be concluded that each of the three stabilizing copolymers gives an identical flocculated network structure.

In Fig 13, the Bingham yield stress is plotted against increasing HEC concentration. Here, unlike the oscillation measurements, differences between the three stabilizing copolymers are found. It can be clearly seen that F108 gives the highest yield stress values while P103 gives the lowest. This correlates with the molar mass of the PEO stabilizing chain, the highest of which gives the greatest yield stress.

Therefore, it is the strength of flocculation that governs the formation of liquid and solid phases. Oscillatory shear measurements can detect the formation of the solid phase, due to its continuous network of particles, while yield stress measurements

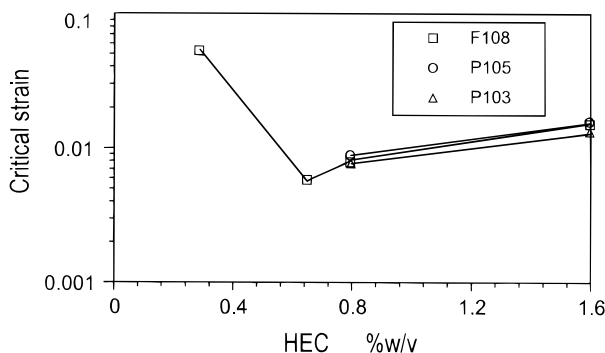


Figure 12. Critical strain (0.5 Hz) as a function of HEC G concentration for a 67 nm latex stabilized with different PEO-PPO-PEO block copolymers.

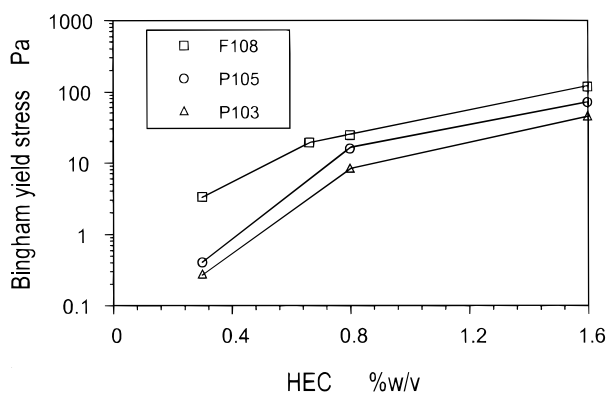


Figure 13. Bingham yield stress as a function of HEC G concentration for a 67 nm latex stabilized with different PEO-PPO-PEO block copolymers.

can detect differences in the strength of the interparticle attraction due to the different stabilizing copolymers, in agreement with the microscopic phase observations.

Consideration of the adsorbed amount and the adsorbed layer thickness together allows the amount of PEO per unit volume in the adsorbed layer to be calculated. Assuming a uniform polymer segment density profile, this gives volume fractions of PEO in the adsorbed polymer layer of 0.044, 0.056 and 0.087 for P103, P105 and F108 respectively. Therefore, the F108 layers are the 'hardest' with the highest concentration of PEO, which strongly repels the HEC coils from the surface of the particles to give relatively thick depletion layers. In contrast, the P103 layers are the 'softest' with the lowest concentration of PEO, which allows considerable penetration by the HEC coils and thus has relatively thin depletion layers. This is illustrated in Fig 14.

It is possible to compare the rheological data with the theory of the depletion interaction proposed by Vincent *et al.*³⁰ According to these authors (VEEJ theory), the strength of the depletion attraction G_{dep} , can be calculated by multiplying the osmotic pressure difference obtained when polymer coils are excluded from the region between two particles by the volume of this polymer depletion zone. This is given by:

$$G_{\text{dep}} = 2\pi a \left(\frac{\mu_1 - \mu_1^0}{v_1} \right) \left(\Delta + \delta - p - \frac{h}{2} \right)^2 \quad (12)$$

where the quantity $\mu_1 - \mu_1^0$ is the free energy change in moving a solvent molecule from pure solvent to

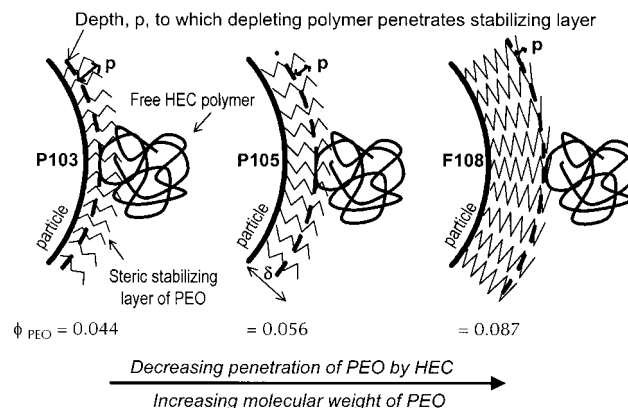


Figure 14. Illustration of the effect of the steric stabilizing layer according to the VEEJ theory.

polymer solution and v_1 the volume of a solvent molecule. These terms describe the osmotic pressure contribution and for the geometrical term relating to the excluded volume, Δ is the hard sphere depletion layer thickness, δ the thickness of the adsorbed polymer layer and a the particle radius. Here the true depletion layer thickness is given by $\Delta + \delta - p$, where Δ is of the order of the size of the HEC coils and p is the depth the free HEC polymer coils penetrate the steric layer. Therefore, it can readily be seen that more penetrable, less dense steric layers will have higher values of p and thinner depletion layers, resulting in weaker flocculation.

The minimum in the interaction energy, $G_{T, \text{min}}$, can be obtained by summing all the interparticle forces thus:

$$G_T = G_{\text{dep}} + G_{\text{el}} + G_{\text{mix}} \quad (13)$$

where G_{el} and G_{mix} are the repulsive elastic and mixing contributions from the steric stabilizing layers. The van der Waals forces were considered to be relatively small at these separations and not included. This may then be compared with the experimental yield stress values through eqn (6).

These data are presented in Table 2 where it can clearly be seen that the strength of flocculation (ie E_{sep}) with F108 is some two to three times stronger than for P103. Comparison of these results with the calculated values ($G_{T, \text{min}}$) gives good correlation with the numerical trends but poor agreement with the actual values. The VEEJ theory overestimates the values for $G_{T, \text{min}}$ but does predict the trend in increasing flocculation strength from P103 to F108. The poor numerical correlation is most likely due to

HEC (g litre ⁻¹)	P103		P105		F108	
	E_{sep}	$G_{T, \text{min}}$	E_{sep}	$G_{T, \text{min}}$	E_{sep}	$G_{T, \text{min}}$
3.0	0.030	5.73	0.044	6.15	0.370	6.72
6.6	—	9.87	—	10.61	2.15	11.68
8.0	0.924	11.03	1.75	11.83	2.77	13.05
16.0	5.50	12.29	7.98	12.78	13.1	13.92

Table 2. E_{sep} (kT) and $G_{T, \text{min}}$ (kT) values for 67 nm latex stabilized with P103, P105 or F108.

the assumptions made in the estimation of E_{sep} , namely the number of contacts per particle, and that these contacts are fully broken under high shear, which may not be the case for particles this small.

The basic philosophy of this theory provides a valuable insight into the mechanism by which the particle softness influences the strength of the attraction in depletion-flocculated suspensions. This is illustrated in Fig 14, where it can be seen that the relatively low-density, soft PEO layers obtained with P103 allow more penetration by the HEC than the harder, high-density PEO layers obtained with F108. It is by this penetration that the volume of the excluded depletion zone, and hence G_{dep} , is reduced with softer stabilizing layers. Furthermore, based on the earlier findings whereby it is the floc network that controls the sedimentation, then the presence of soft layers will result in a weaker network which could sediment more rapidly.

3.4 Molecular mass effects on non-adsorbing polymer

In this experiment, the sedimentation behaviour of a series of SCs containing fluquinconazole with polymers of different molecular mass were examined. The concentration range for each polymer was chosen to cover similar sedimentation rates so that direct comparisons could be made. The resulting sedimentation rates are shown in Fig 15, with the initial sedimentation rate indicated by dashed lines and the long-time sedimentation rate shown as solid lines.

Two molecular mass effects of the polymer are visible. First, the presence of two sedimentation rates is more pronounced with lower molecular masses and second, higher molecular mass polymers are more effective at preventing sedimentation, as would be expected from the stronger depletion effect.

To examine the rheological correlation, one sample for each polymer with an initial sedimentation velocity of 3 mm day^{-1} was examined. This initial velocity was chosen since it is the network structure in

these samples which is also present within the samples inside the rheometer cell. The resulting stress relaxation curves are shown in Fig 16. Interestingly, there is a large difference between the polymers, with the relaxation modulus decreasing with increasing molecular mass. This tells us that the elasticity, and hence the extent of the network structure due to the aggregated particles, is less for the higher-molecular-mass polymers. This is an interesting finding in the light of the earlier experiments which revealed the role of the floc network in preventing sedimentation. If the floc network were the only factor relevant to sedimentation, then the relaxation curves for each of these samples should coincide. The fact that they do not means that the polymer is also a significant factor in the sedimentation process of such systems. This difference in the rheology is also seen with the zero shear viscosity (Fig 17) which, intuitively, might be expected to correlate with the sedimentation rate. This lack of correlation with the zero shear viscosity, obtained from both creep and stress relaxation measurements, has also been observed with other SCs within our laboratory and is not just confined to the results presented here.

By careful analysis of the other rheological parameters, which are also shown in Fig 17, it is possible to extract further information. The most pertinent of these is the elastic limit, since this tells us more about the network. From the elastic modulus we already know that the number of network chains permeating through the sample decreases with increasing molecular mass. The increase in the elastic limit tells us that the network chains are also becoming more tortuous as they decrease in number. We can understand what is happening here by considering how the networks originally form. Simulation of particle aggregation shows that particles initially aggregate into small clusters. Then, as the number of free particles decreases and the clusters grow in size, the clusters themselves aggregate until a continuous network is formed which permeates throughout the whole sample volume. Now consider what the effect

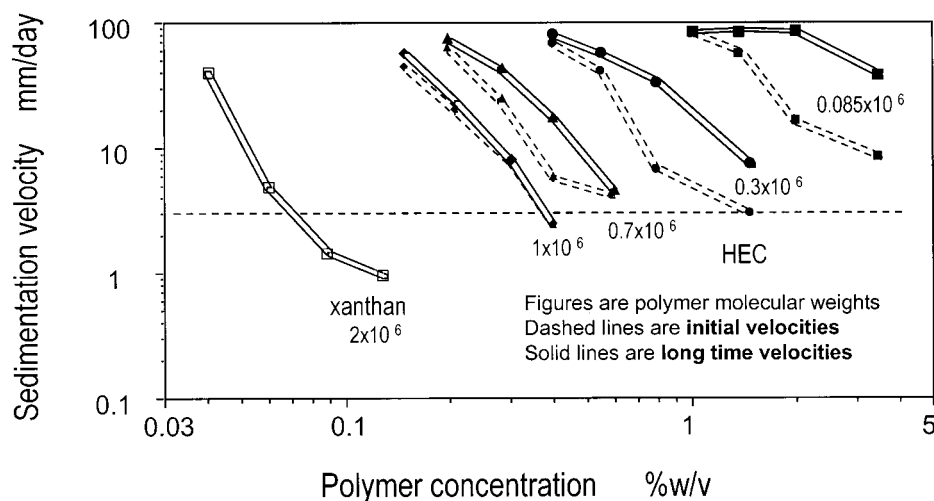


Figure 15. Sedimentation of fluquinconazole SCs containing different molecular mass grades of HEC and xanthan.

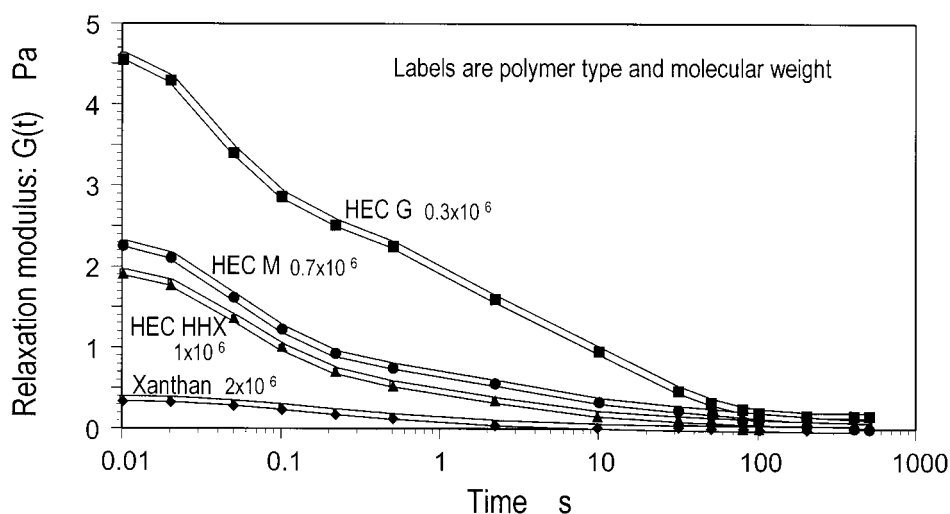


Figure 16. Stress relaxation data for fluquinconazole SCs with a sedimentation rate of 3 mm day^{-1} .

would be if large polymer molecules existed between the aggregating clusters. In cases where the polymer molecules were situated directly between two approaching clusters, aggregation could be prevented. When extrapolated to many clusters simultaneously aggregating, the presence of large polymer molecules could reduce the number of cluster-cluster links formed, such that a cluster may have, for example, only two such links instead of three. If we were to compare each of these cases, then, in a polymer-free system, or a system with small polymer molecules, each cluster would have a relatively high number of cluster-cluster links. However, in a system containing large polymer molecules, each cluster would have fewer cluster-cluster links and the resulting chains would be more tortuous. This is illustrated in Fig 18. Furthermore, in agreement with the reduction in the degree of flocculation observed here, the yield stress also decreases as the molecular mass of the depleting polymer increases, reflecting the decreasing value of the elastic modulus.

The resulting structure of the flocculated network of particles and dispersed polymer molecules may also explain the lack of height dependence observed in aqueous xanthan-based suspensions (Fig 1) since, in order for the network to consolidate and collapse at its base, the free volume between the particulate network clusters must be available for the clusters to collapse into. In a liquid medium this is the case, since any liquid can readily escape through the pores between clusters. However, when large polymer molecules are present, they have nowhere to escape to and are essentially trapped within the particulate network. Here, the network can only collapse when these polymer molecules have slowly diffused out of the network and this offers an explanation as to why larger polymer molecules are more effective at preventing sedimentation. Since this diffusion process does not depend on the total height of the network in the sample, but on the size of the polymer molecule and the size of the pores between the surrounding clusters, the sedimentation rate would not be expected to show any height dependence either.

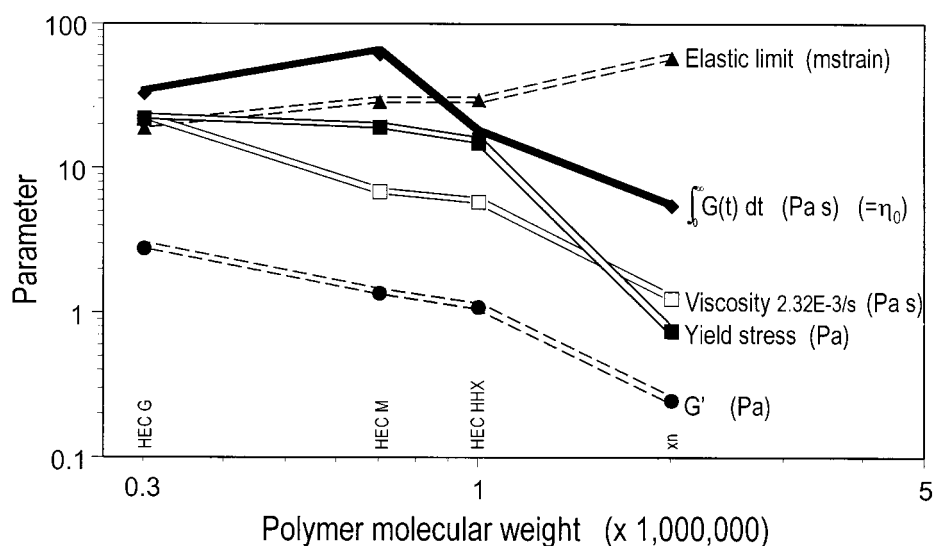


Figure 17. All rheological parameters for the samples shown in Fig 16.

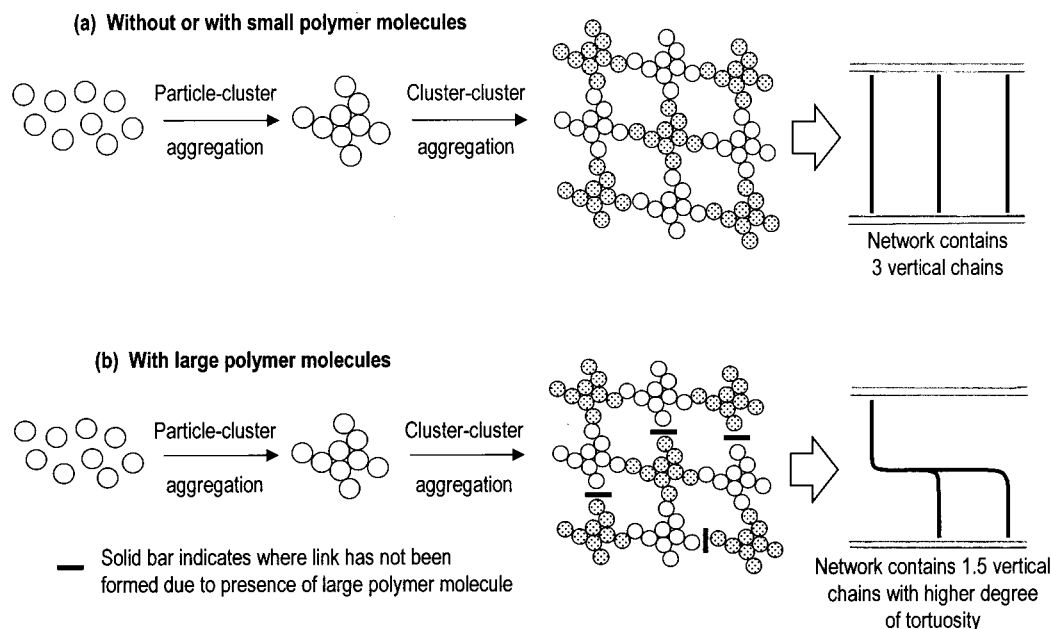


Figure 18. Illustration of the effect of polymers in preventing the formation of cluster–cluster links during aggregation.

Another explanation for these effects could be due to the changes in the attractive depletion interaction between particles with each of the polymers. In this experiment both the depth and range of the depletion attraction vary; the size of the polymer coil in solution governs its range while the polymer concentration governs its depth. Hence, for the same mass of polymer, HEC G has a shorter, deeper-attractive ‘well’ while xanthan has a longer, shallower-attractive ‘well.’ This could affect the structure and strength of the flocs. Unfortunately, due to the range of particle sizes and shapes present with this SC, meaningful calculations are not possible and further experiments with monodisperse latex dispersions will be required. However, the sedimentation results (Fig 15) do show that, in each case, an open, diffusion-limited network structure exists and hence it appears that the flocs are sufficiently strong for flocculation to have occurred via a diffusion-limited mechanism, resulting in a similar network structure for each suspension.

Finally, it is worth considering how much more effective xanthan appears to be in Fig 15 than would be expected for HEC of equivalent molecular mass. For example, if the xanthan data in Fig 17 were fitted to straight lines extrapolated from the HEC data, then the xanthan would need a molecular mass in excess of 5×10^6 . This performance advantage of xanthan can be attributed to its tendency to self-associate into dimers or larger structures³¹ giving it a much higher effective molecular mass.

CONCLUSIONS

Rheological and sedimentation measurements show that it is the formation of a floc network by depletion flocculation that controls the sedimentation in polymer-thickened SCs. Consequently, properties

related to the dispersed phase in SCs, such as particle size, particle concentration and particle softness, alongside the depletion interaction from non-adsorbing polymers, can be important in dictating the properties of SCs. Furthermore, the presence of large, non-adsorbing polymers in agricultural suspension concentrates is also a significant factor in the sedimentation process. Rheological measurements show that, when large polymers are present, the elasticity of the sample is reduced while the sedimentation rate remains constant. Viscoelastic measurements indicate that this is due the polymer partially blocking the formation of the floc network. Also, there is no direct correlation between rheology and sedimentation, even with zero shear viscosity. It is postulated that the sedimentation rate is governed by the rate at which the non-adsorbing polymer molecules can diffuse through the floc network before the particle clusters in the network can rearrange and sedimentation occurs.

ACKNOWLEDGEMENTS

We would like to thank Y. Kamata and H Innami for their assistance with some of the sedimentation measurements and the management of AgrEvo for permission to publish this work.

REFERENCES

- 1 Symes KC, The relationship between the covalent structure of the Xanthomonas polysaccharide (xanthan) and its function as a thickening suspending, and gelling agent. *Food Chemistry* 6:63–76 (1980).
- 2 Clark RC and Lockwood B, Use of microbial polysaccharides in the formulation of stable suspensions. *17th Japan Agricultural Formulation and Application Symposium* 30–31 October 1997, Conference booklet. Japanese Agricultural Society. p 59 (1997).

- 3 Howe AM and Robins MM, Determination of gravitational separation in dispersion from concentration profiles. *Colloids and Surfaces* **43**:83–94 (1990).
- 4 Wedlock DJ, Moman A and Grimsey J, Consolidation of depletion flocculated concentrated suspensions. Influence of non-adsorbing polymer concentration on consolidation rate constants. *Colloids and Surfaces* **54**:125–134 (1991).
- 5 Buscall R, The sedimentation of concentrated colloidal suspensions. *Colloids and Surfaces* **43**:33–53 (1990).
- 6 Kynch GF, A theory of sedimentation. *Trans Faraday Soc* **48**:166–167 (1952).
- 7 Richardson JF and Zaki WN, Sedimentation and fluidization. *Trans Inst Chem Eng* **32**:35–53 (1954).
- 8 Maude AD and Whitmore RL, Generalised theory of sedimentation. *Brit J Appl Phys* **9**:477–488 (1958).
- 9 Michaels AS and Bolger JC, Settling rates and sediment volumes of flocculated kaolin suspensions. *Ind Eng Chem Fund* **1**:24–33 (1962).
- 10 Buscall R, Mills PDA, Goodwin JW and Lawson DW, Scaling behaviour of the rheology of aggregates networks formed from colloidal particles. *J Chem Soc Faraday Trans 1* **84**:4249–4259 (1988).
- 11 Buscall R and McGowan I, Sedimentation and viscous flow of weakly flocculated concentrated dispersions. *Far Disc Chem Soc* **76**:277–290 (1982).
- 12 Partridge, SJ, Rheology of cohesive sediments, *PhD, Thesis*, University of Bristol (1985).
- 13 Tadros ThF and Zsednai A, Application of depletion flocculation for prevention of formation of dilatant sediments. *Colloids and Surfaces* **43**:105–116 (1990).
- 14 Buscall R, Goodwin JW, Ottewill RH and Tadros ThF, The settling of particles through Newtonian and non-Newtonian media. *J Coll Interface Sci* **85**:78–86 (1982).
- 15 Wedlock DJ, Barker A, Grimsey J and Moman A, Consolidation of depletion flocculated concentrated suspensions, influence of non-adsorbing polymer concentration, in *Adv Meas Control Colloidal Processes*, ed by Williams RA and De Jaeger NC, Butterworth-Heinemann, Oxford, pp 51–64 (1991).
- 16 Goodwin JW, Hearn J, Ho CC and Ottewill RH, Preparation and characterization of polymer latices formed in the absence of surface active agents. *Brit Polym J* **5**:347–362 (1973).
- 17 Goodwin JW, Hearne J, Ho CC and Ottewill RH, Preparation and characterization of polymer latices formed in the absence of surface active agents. *Colloid Polym Sci* **252**:464–471 (1974).
- 18 Faers MA and Luckham PF, Effect of steric stabilizing layer on the phase behavior and rheology of small polystyrene latex dispersions induced by changes to the concentration of nonadsorbing hydroxyethylcellulose. *Langmuir* **13**:2922–2931 (1997).
- 19 Faers MA and Luckham PF, Rheology of polyethylene oxide-polypropylene oxide block copolymer stabilized latices and emulsions. *Colloids and Surfaces A* **86**:317–327 (1994).
- 20 Gillespie J, An extension of Goodevee's impulse theory of viscosity to pseudoplastic systems. *J Coll Sci* **15**:219–231 (1960).
- 21 Luckham PF, Vincent B and Tadros ThF, The controlled flocculation of particulate dispersions using small particles of opposite charge. III. Investigation of floc structure using rheological techniques. *Colloids and Surfaces* **6**:101 (1983).
- 22 Asakura S and Oosawa F, Surface tension of high-polymer solutions *J Chem Phys* **22**:1255 (1954).
- 23 Asakura S and Oosawa F, Interaction between particles suspended in solutions of macromolecules. *J Polym Sci* **33**:183–192 (1958).
- 24 Gast AP, Russel WB and Hall CK, An experimental and theoretical study of phase transitions in the polystyrene latex and hydroxyethylcellulose system. *J Coll Interface Sci* **109**:161–171 (1986).
- 25 Meakin P, Formation of fractal clusters and networks by irreversible diffusion-limited aggregation. *Phys Rev Lett* **51**:1119–1122 (1983).
- 26 Kolb M, Botet R and Julien R, Scaling of kinetically growing clusters. *Phys Rev Lett* **52**:1123–1126 (1984).
- 27 Brown WD and Ball RC, Computer simulation of chemically limited aggregation. *J Phys A* **18**:L517–L521 (1985).
- 28 Sonntag RC and Russel WB, Elastic properties of flocculated networks. *J Coll Interface Sci* **116**:485–489 (1987).
- 29 Lekkerkerker HNW Poon WCK, Pusey PN, Stroobants A and Warren PB, Phase-behavior of colloid plus polymer mixtures. *Europhys Lett* **20**:559–564 (1992).
- 30 Vincent B, Edwards J, Emmett S and Jones A, Depleted flocculation in dispersions of sterically-stabilized particles (soft spheres). *Colloid and Surfaces* **18**:261–281 (1986).
- 31 Meyer EL, Fuller GG, Clark RC and Kulicke WM, Investigation of xanthum gum solution behavior under shear-flow using rheological techniques. *Macromolecules* **26**:504–511 (1993).